

Erik Stacey^{1, 2}, Gregg A. Wade^{1, 2}, James Barron²

¹Dept. of Physics, Engineering Physics and Astronomy, Queen's University, Kingston, ON

²Dept. Of Physics and Space Science, Royal Military College of Canada, Kingston, ON

Context

Plaskett's Star (HD 47129) is a massive ($\sim 100 M_{\odot}$), short-period ($P = 14.396257d$) non-eclipsing spectroscopic binary consisting of an O8 primary component and an O7.5 secondary component (Linder et al. 2008). Recently, scientific interest in this system has been stoked by the discovery of a strong (kG) magnetic field in the rapidly rotating ($P_{rot} = 1.21551_{-34}^{+28} d$; Grunhut et al. 2020) secondary star and a lack of radial velocity variation in its broad spectral lines (Grunhut et al. 2020 and poster by Folsom et al., this conference).

The *Transiting Exoplanet Survey Satellite* (TESS) project has released high-precision photometry of HD 47129 as a part of its sector 6 targeted component. The data products all span approximately 21.7 days and include 2-minute cadence light curves with and without camera-wide detrending applied (the former shown in Fig. 1, and the latter corresponding to the *simple aperture photometry*, or SAP), and 30-minute cadence full-frame images.

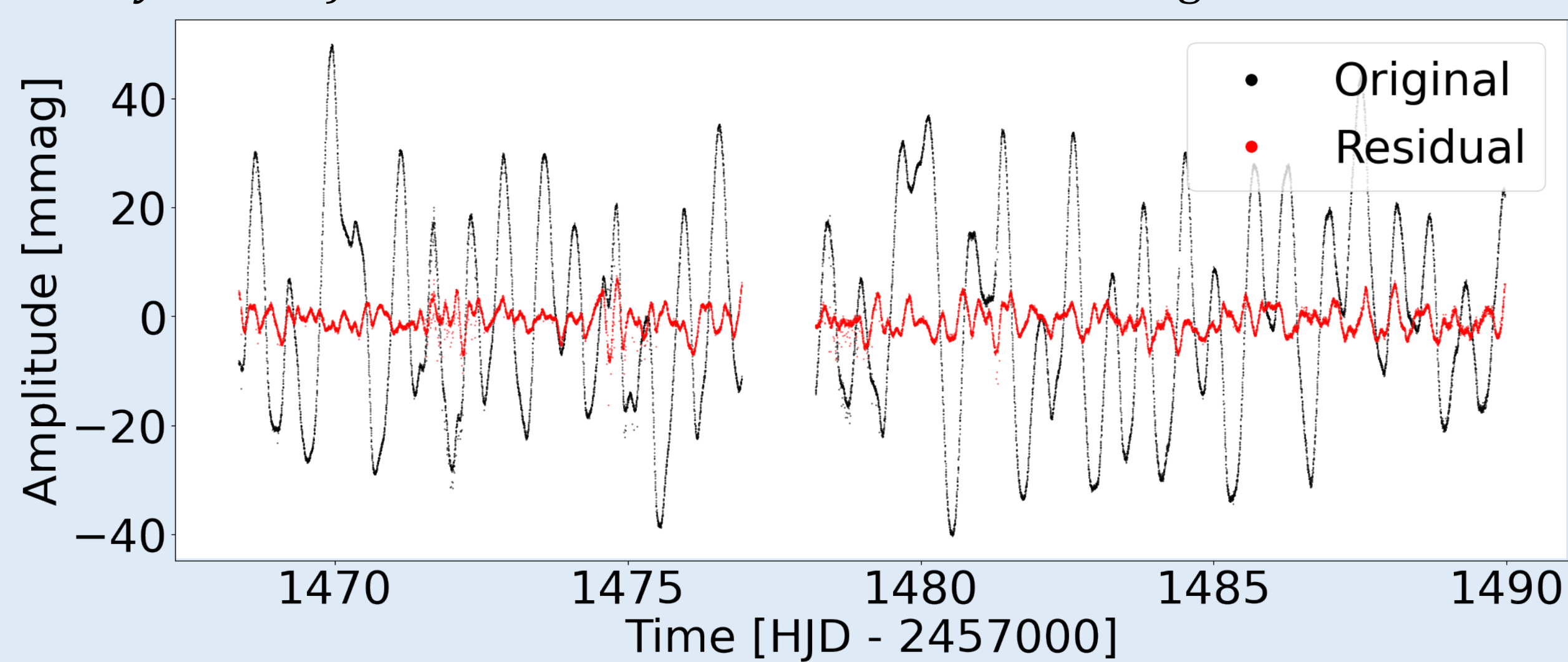
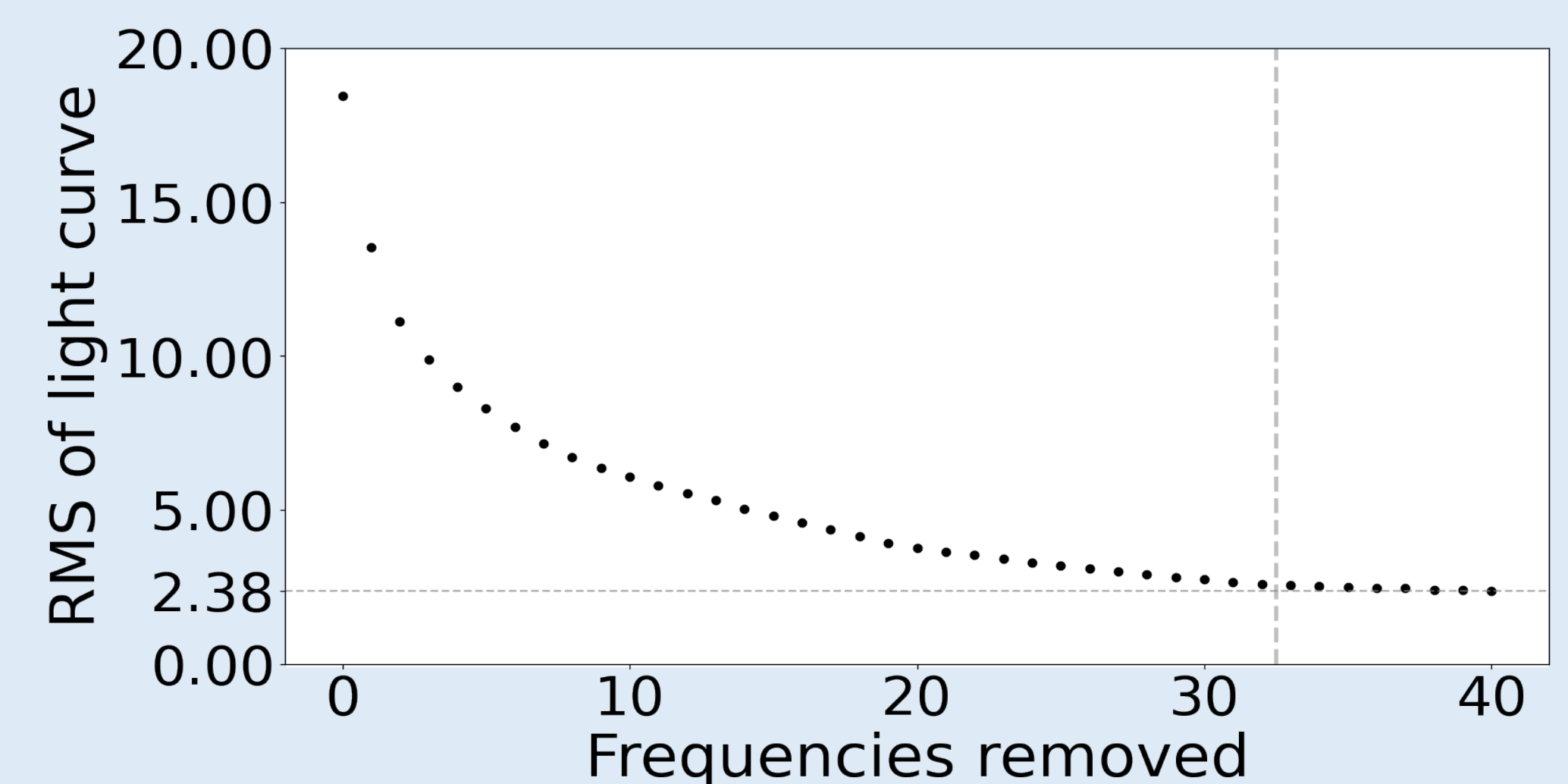


Fig 1: The reduced TESS differential light curve of Plaskett's Star (black) and the residual light curve after removing 40 frequencies (red).

Method

We used a novel Lomb-Scargle-based, Python-implemented iterative pre-whitening routine to identify individual periodic components. For each iteration, a Lomb-Scargle periodogram was computed to identify the frequency with the highest amplitude, then a least-squares sinusoidal fit was performed to the data at the target frequency. The fit was subtracted and the process iterated. After 32 periodic components were identified, peaks were selected according to highest amplitude exceeding a degree-5 polynomial fit to the periodogram in log-log space by a factor of 3 or more. If no peaks met this condition, the pre-whitening was terminated.

Fig 2: The standard deviation of the residual light curve at each pre-whitening iteration. The vertical dashed grey line indicates the change of peak selection method.



After removing 40 frequencies, we assumed the remaining variability in the light curve to be noise and approximated it with a final polynomial fit. Using this model, we assessed the significance of each peak through comparison with the fitted amplitude. Only frequencies with amplitudes exceeding the local noise level by a factor of four are considered statistically significant.

Results

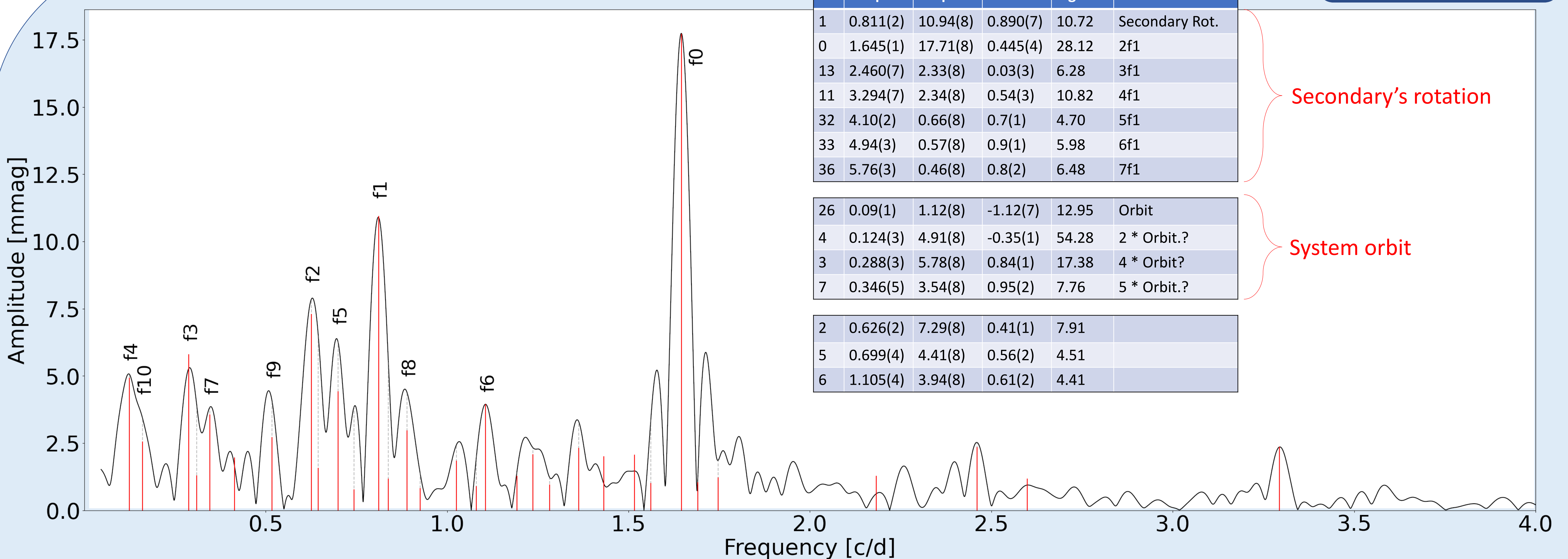


Fig 3: The periodogram of the reduced light curve. Vertical red lines are present at the location of extracted periodic components, with height corresponding to the fitted amplitude. The inset tables highlight frequencies of interest from the reduced light curve, due to their association with a known source of variability or large amplitude.

We identified 35 formally significant frequencies in the reduced light curve, 34 in the SAP light curve, and 39 in the 30-minute FFI light curve. We detected a harmonic structure composed of the broad-lined star's rotational frequency at $0.8111 \pm 0.24 c/d$ and harmonics up to the sixth. The first harmonic in this structure has a substantially higher amplitude than the fundamental. This phenomenon is likely due to a corotating centrifugal magnetosphere with two dense clouds confined to two potential minima symmetric about the magnetic axis. As the baseline of the light curve falls just shy of spanning two orbital cycles, our ability to probe very low power ($\approx 0.1 c/d$) frequencies was limited. Despite this, we detect what appears to be a harmonic structure about the orbital frequency of the system at $0.09 \pm 0.01 c/d$ consisting of the fundamental and the first, third, and fourth harmonics.

Aside from the secondary's rotation and the system orbit, we also expect to observe

variability due to the *primary* star's rotation. Grunhut et al. (2013) provided an inferred estimate for this period of $\frac{P}{\sin i} = 10.2 \pm 4$ days ($0.1 \pm 0.04 c/d$) based on the temperature and luminosity of the star and the broadening observed in its spectral lines. This is unlikely to account for the strong variability we see at 0.626, 0.699, and 1.105 c/d, however it is in the realm of the system's orbital frequency and could be conflated with or aligned to this variability.

Burssens et al. (2020) provides frequency analyses of O and B-type stars in TESS sectors 1-13, which includes HD 47129. Using a substantially more conservative iterative pre-whitening process, they detect 9 frequencies for this system all of which are detected in our analysis within error.

Between this analysis, that of Burssens et al. (2020), and the CoRoT photometry and analysis by Mahy et al. (2011), the photometric variability of Plaskett's Star has been extensively characterized and will serve to inform further study of this enigmatic system.

References

- Grunhut et al., 2013, MNRAS, 428, 1686
 Linder et al., 2008, A&A, 489, 713
 Grunhut et al., 2020, pending publication
 Burssens et al., 2020, pending publication
 Mahy et al. 2013, A&A, 525, A101